IOP Publishing Journal of Physics: Condensed Matter
J. Phys.: Condens. Matter **25** (2013) 495506 (7pp) doi:10.1088/0953-8984/25/49/495506

Effects of Ni vacancies and crystallite size on the O 1s and Ni 2p x-ray absorption spectra of nanocrystalline NiO

R J O Mossanek[1], G Domínguez-Cañizares[2], A Gutiérrez[2], M Abbate[1], D Díaz-Fernández[2] and L Soriano[2]

[1] Departamento de Física, Universidade Federal do Paraná, Caixa Postal 19044, 81531-980 Curitiba-PR, Brazil
[2] Departamento de Física Aplicada and Instituto de Ciencia de Materiales Nicolás Cabrera, Universidad Autónoma de Madrid, Cantoblanco, E-28049 Madrid, Spain

E-mail: a.gutierrez@uam.es

Received 2 September 2013, in final form 4 October 2013
Published 8 November 2013
Online at stacks.iop.org/JPhysCM/25/495506

Abstract
We have studied the electronic structure of nanocrystalline NiO thin films, grown by radio-frequency magnetron sputtering under different experimental conditions, using x-ray absorption spectroscopy. The O 1s and Ni 2p spectra showed distinct changes as a function of O_2 content in the plasma, which were reproduced with cluster model calculations. These changes are attributed to the incrementing of the surface contribution due to a decrease of the crystallite size as the O_2 content in the plasma increases, and to the presence of induced nickel vacancies. Thus, the changes in the electronic structure can be related to the modification of structural and transport properties of these nanocrystalline films.

(Some figures may appear in colour only in the online journal)

1. Introduction

NiO is one of the most studied transition metal oxides, not only in fundamental physics, but also for practical purposes. In recent years there have been many works proposing the use of NiO in technological applications such as electrochemical capacitors and supercapacitors [1, 2], electro-optical devices [3, 4], electrochromism [5], electrodes in lithium batteries [6], and devices based on resistive switching [7]. Nanostructured NiO is especially attractive because of its higher effective surface [8], which ends up yielding unique properties for current applications such as catalysis [9] and energy conversion and storage [10].

The physical properties of any material, and thus the actual feasibility of its application, strongly depend on the stoichiometry, density of defects, and crystallinity, which are very sensitive to the growth parameters. Previously, we have grown NiO films and membranes by magnetron sputtering with tailored properties, and shown that changes in the conductivity, due to the presence of vacancies, could be achieved by modifying some of the deposition parameters [11].

Nevertheless, valuable insight can be obtained by studying the electronic structure of these systems. Then, the changes in the physical properties can be directly related to their microscopic origin, although theoretical studies are required to confirm structural assumptions. In previous works, we showed that the Ni 2p x-ray photoelectron spectral line shape of NiO is influenced by surface effects [12, 13]. These effects are enhanced when the surface-to-volume ratio increases, as in nanostructured NiO [14, 15], and are also present in the O 1s x-ray absorption spectra (XAS) of NiO [16, 17].

X-ray absorption spectroscopy is a suitable technique to use to study the electronic structure in this case, because it is very sensitive to the chemical environment and gives information on the covalent character of bondings and on the ground state and symmetry of a specific ion. This method was already applied for studying the electronic structure of

Li-doped NiO [18, 19], and that of the nickel perovskites $LaNiO_3$ [20] and $PrNiO_3$ [21].

We present here x-ray absorption spectroscopy results on a series of nanocrystalline NiO thin films grown by RF magnetron sputtering with different oxygen-to-argon ratios in the plasma during deposition. The O 1s edge showed significant changes as a function of oxygen content in the plasma, whereas the Ni 2p edge presented only minor modifications. We were able to explain the distinct changes in both XAS spectra with theoretical cluster model calculations. The systematic changes in the electronic structure of these thin films are attributed to the enhancement of the surface contribution, as well as to the presence of nickel vacancies, which induce the formation of Ni^{3+} states. These effects can help to explain the changes in the conductivity of nanostructured NiO films with different growth conditions [11].

2. Experimental details

NiO thin films were grown by RF magnetron sputtering of a NiO target (AJA International, 99.95% purity) on single-crystal silicon wafers (p-type with (100) orientation). The deposition was carried out at room temperature in a high vacuum chamber with a base pressure below 10^{-7} mbar. The pressure used for plasma ignition was 1.5×10^{-2} mbar, and was maintained at this value during the whole growth process, which took about one hour. The plasma was composed of a mixture of oxygen and argon, with an oxygen content ranging from 0% to 100%. The substrates were rotated during deposition at about 10 rpm in order to obtain a more uniform film. The angle of the sputtering cathode was 23° (off-axis) with respect to the normal of the substrate surface, and the distance between the target and substrate was 8 cm. Before starting deposition a pre-sputtering of 5 min was performed in order to clean the target surface. The magnetron power was set to 200 W. Although no heating was applied, a temperature increase of about 50 °C, induced by the plasma, was observed in the surface of the substrates at the end of the deposition, as was monitored by an IR external pyrometer operating through a sapphire window. The NiO films grown in this way were polycrystalline, with thickness between 100 and 240 nm, as determined with a Dektak 150+ Surface Profiler from Veeco. The electrical resistivity of the films was measured at room temperature by the Van der Pauw method using an Ecopia HMS-5000 system.

X-ray diffraction (XRD) measurements were carried out with a Panalytical Xpert PRO diffractometer in a grazing incidence condition. In the setup used, an x-ray tube providing Cu Kα radiation with the corresponding optical setup provides a parallel and monochromatic x-ray beam. XRD data were collected with a beam incidence angle of 1° and a 2θ scan between 30° and 70° with a step size of 0.03°and a counting time of 5 s/step.

The O 1s and the Ni 2p x-ray absorption spectra were obtained at the Optics Beamline of the BESSY II synchrotron radiation source in total electron yield mode by measuring the sample drain current. The photon energy was calibrated comparing the binding energy of the Au $4f_{7/2}$ photoemission peak excited with first-order and second-order light. The energy resolution was approximately 100 meV at a photon energy of about 500 eV. The spectra were recorded under normal incidence, and were normalized using a spectrum from a fresh gold sample in order to correct the spectra for the contamination of the optical elements and other possible artefacts.

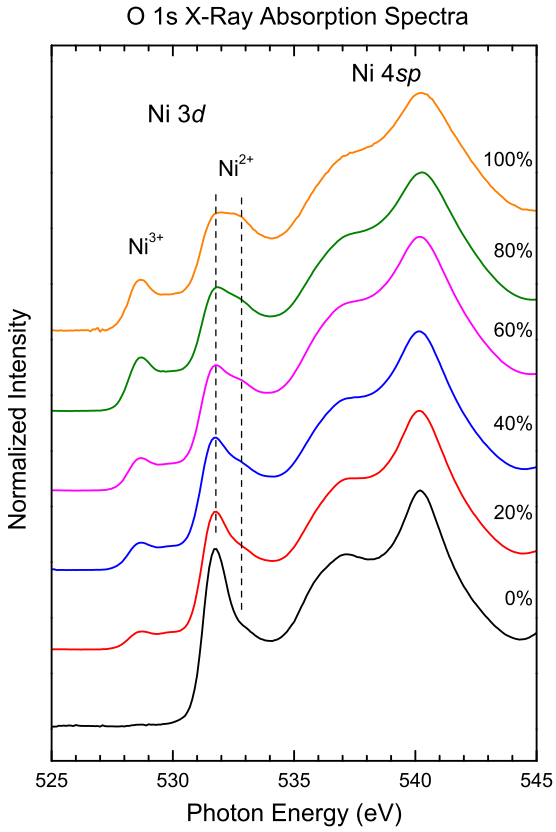

Figure 1. O 1s x-ray absorption spectra of NiO thin films as a function of O_2 content in the sputtering plasma during growth. The spectra show empty O 2p states covalently mixed with Ni 3d and Ni 4sp states. The increase of O_2 content produces a Ni^{3+} contribution and a splitting of the Ni^{2+} states.

3. Results and discussion

3.1. O 1s x-ray absorption spectra

Figure 1 shows the experimental O 1s x-ray absorption spectra of samples with different growth conditions. The spectrum for the sample with no O_2 content (0%) is in very good agreement with previous spectra for bulk NiO [18, 22–24]. The absence of O_2 during the sputtering deposition could lead to a decrease in the oxygen content of the films, and hence to partially reduced NiO. This would be evidenced by the presence of metallic Ni in the films. However, no traces of metallic Ni were observed either in the XAS spectra or through XPS, as reported elsewhere [25]. The structures observed in figure 1 are related to empty O 2p states covalently mixed with Ni^{2+} 3d states, at around 532 eV, and with Ni 4sp

states, above 535 eV. The small component, around 533 eV, is attributed to the splitting of Ni 3d orbitals, due to surface effects [16].

When samples are grown in the presence of O_2, on the other hand, there is a change in the Ni 3d region of the spectra. The surface related contribution, at about 533 eV, becomes more prominent, and a new feature appears, at around 529 eV. This new peak is attributed to O 2p states mixed with Ni^{3+} 3d states [18]. The relative intensity of these features indicates that the O_2 content during growth causes two effects: (i) an increase in the surface-to-bulk ratio in the samples, and (ii) a further oxidation of nickel ions.

The first effect is attributed to the diminution of crystalline size when the oxygen content in the plasma increases. Figure 2 shows x-ray diffraction (XRD) patterns in the region of the NiO (220) peak for samples grown with different oxygen contents in the plasma. A small shift towards lower angles can be observed, which suggests an increase in the lattice parameter due to an excess oxygen in the lattice, as discussed in previous works [11]. The peak width clearly broadens as the oxygen content increases, which, according to the Scherrer analysis, indicates that the addition of oxygen to the plasma produces a grain size reduction. A simple analysis gives a decrease in the average grain size from about 30 nm for the sample grown with pure Ar to less than 10 nm for the sample grown with pure O_2. Further, this effect has also been directly observed by scanning electron microscopy [25].

On the other hand, the increase of the pre-edge feature in the O 1s XAS spectra, attributed to Ni^{3+} states, can explain the increase of the electrical conductivity of the NiO films with the oxygen content in the plasma during growth. In figure 3 we show the electrical resistivity of the NiO films as a function of the oxygen content of the plasma. A clear decreasing trend can be observed in a range that covers more than two orders of magnitude. This trend has already been observed in the past [3, 11, 26]. In a previous work we showed that the observed decrease in resistivity is correlated with a decrease in the Ni–Ni coordination number observed via EXAFS [11], which is an evidence of the presence of Ni vacancies in the films. This correlation suggests that the electrical behaviour of the NiO films is based on the conduction by holes.

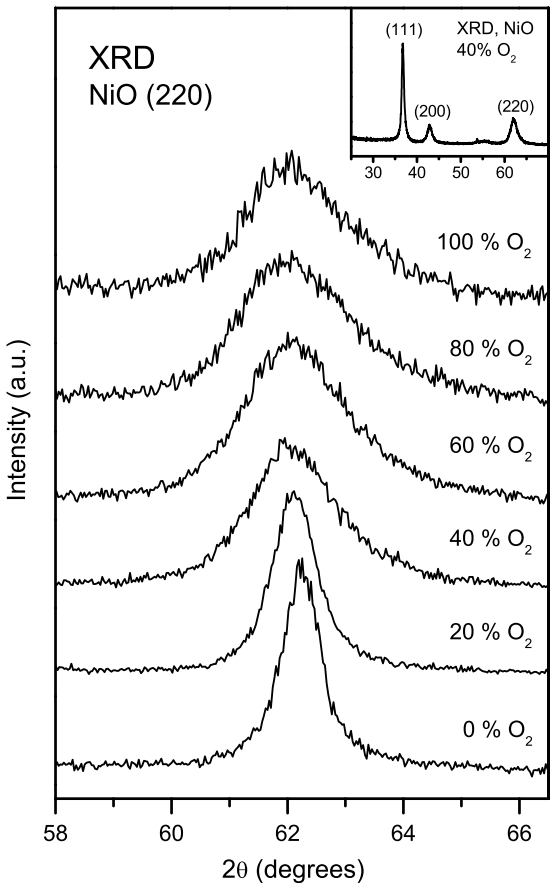

Figure 2. X-ray diffraction patterns around the (220) peak of NiO samples grown with different oxygen contents in the plasma. The inset shows, as an example, the complete diffraction pattern for the 40% sample, which is typical of NiO.

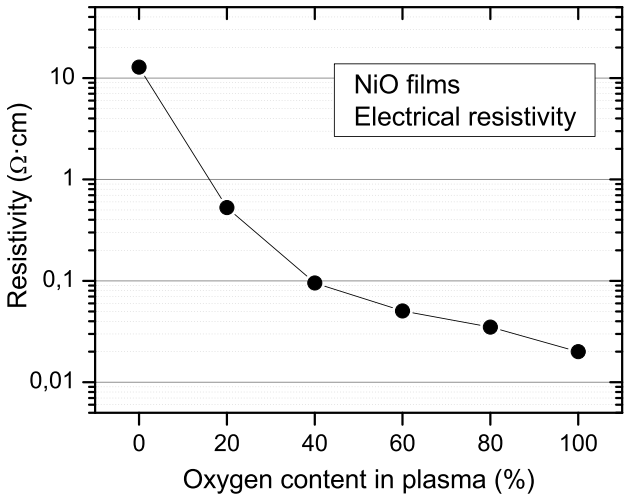

Figure 3. Evolution of the electrical resistivity of NiO films grown on different substrates with the oxygen content in the sputtering plasma.

3.2. Cluster model calculations

In order to confirm the origin of the features in the O 1s XAS spectra, we have performed cluster model calculations. The model consisted of a regular octahedral NiO_6 or pyramidal NiO_5 cluster, solved with the standard configuration interaction method [27, 28]. The ground state wavefunction is expanded in the $3d^n$, $3d^{n+1}\underline{L}$, $3d^{n+2}\underline{L}^2$, etc configurations, and the addition state wavefunction is expanded in the $3d^{n+1}$, $3d^{n+2}\underline{L}$, $3d^{n+3}\underline{L}^2$, etc configurations, where $\underline{L}$ denotes a hole in the ligand (oxygen) band. Finally, the spectral weight is calculated within the sudden approximation.

The main parameters of the model are the charge transfer energy Δ, the d–d Mott Hubbard repulsion U, and the p–d transfer integral pdσ [29]. Each configuration is further split by multiplet effects, given in terms of the Racah parameters B and C, and the crystal field splitting $10Dq$. The values used in the calculations are listed in table 1, and are similar

Table 1. Cluster model parameters (all values in eV).

	Ni^{2+}	Ni^{3+}
Δ	4.0	1.0
U	7.5	7.0
pdσ	1.5	1.8
B	0.13	0.16
C	0.58	0.60
$10Dq$	1.0	1.2

to those from previous works on NiO [13, 14, 30] and on (Pr)$LaNiO_3$ [20, 21].

Calculations for a Ni^{2+} or a Ni^{3+} ground state ionic configuration were done separately. In the case of Ni^{2+}, two contributions were considered: (i) a bulk contribution, where nickel ions appear in octahedral symmetry (NiO_6) [13], and the interaction between p–d electrons in the e_g band is given by $T_\sigma = \sqrt{3}pd\sigma$; and (ii) a surface contribution, where nickel ions appear in pyramidal symmetry (NiO_5) [13], and the interaction between p–d electrons is split into $T_{basal} = T_\sigma$ and $T_{apical} \approx 0.6T_\sigma$ due to the absence of an apical oxygen [13].

In the case of Ni^{2+} calculations, the ground state is composed of about 79% of $3d^8$, 20% of $3d^9\underline{L}$ and 1% of $3d^{10}\underline{L}^2$ configurations, depending on the chosen symmetry. On the other hand, the Ni^{3+} calculation shows a ground state formed from 34% of $3d^7$, 58% of $3d^8\underline{L}$, 7% of $3d^9\underline{L}^2$ and 1% of $3d^{10}\underline{L}^3$ configurations. It is worth noting that the latter is in the negative charge transfer regime because of the larger $3d^{n+1}\underline{L}$ contribution, and that the $3d^7$ configuration is actually in a low spin state ($t^3_{2g\uparrow}t^3_{2g\downarrow}e^1_{g\uparrow}$), as in the case of $LaNiO_3$ [20]. These results will be essential for explaining all the spectra.

Figure 4 presents the O 1s x-ray absorption spectra calculated in the case of octahedral Ni^{2+}, pyramidal Ni^{2+}, and Ni^{3+} ions. The relative energies of the discrete final states were preserved, but the absolute energy scale was adjusted/shifted to get the best agreement with the O 1s absorption edge. Finally, the calculated transitions were convoluted with a 0.3 eV Lorentzian and a 0.5 eV Gaussian function, to simulate lifetime and experimental broadening effects, respectively.

The Ni^{2+} calculations show final states mainly related to the $3d^9$ configuration. In octahedral symmetry, there is only one structure, at 531.8 eV, related to the addition of an electron in the e_g sub-band. In pyramidal symmetry, the e_g degeneracy is split into two contributions, at 532.4 and 533.0 eV, which are due to the addition of an electron in the apical (z^2) or basal (x^2-y^2) sub-bands. The Ni^{3+} calculations are similar to those in previous reports [20] and show final states mainly related to the $3d^8$ configuration. The structures appear at lower energies than in the Ni^{2+} case, at around 528.6, 529.5 and 530.3 eV, and are attributed to the addition of different majority or minority spin e_g electrons, because of the low spin state of Ni^{3+} ions.

Figure 5 shows the calculated O 1s x-ray absorption spectra of samples with different growth conditions. The total spectra are the sums of the calculated octahedral Ni^{2+}, pyramidal Ni^{2+}, and Ni^{3+} contributions, which were weighted (see the inset) in order to give the best agreement with the experimental results.

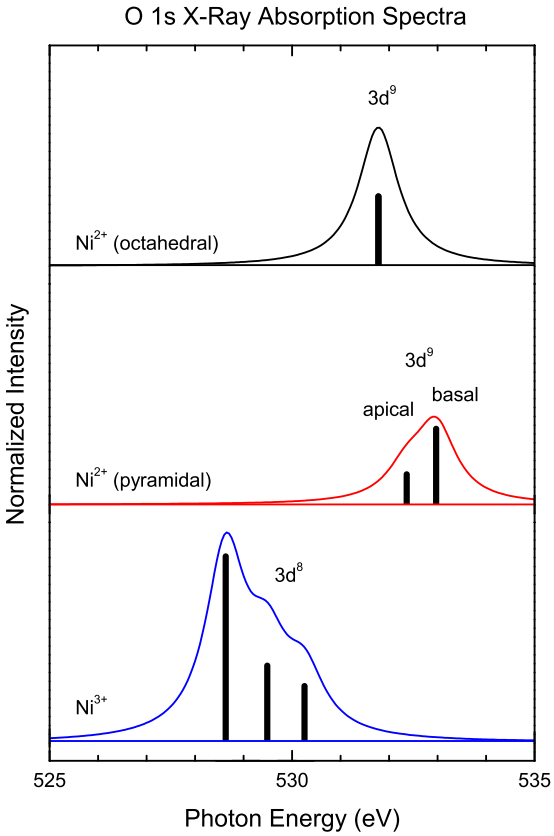

Figure 4. Calculated O 1s x-ray absorption spectra for octahedral Ni^{2+}, pyramidal Ni^{2+}, and Ni^{3+} ions.

The spectrum for the sample with no O_2 content is formed only from Ni^{2+} contributions, 60% in octahedral (bulk) and 40% in pyramidal (surface) symmetries. In contrast, the spectrum of the sample grown with 100% O_2 content is formed from 14% of Ni^{3+} and 86% of Ni^{2+} contributions, which are split into 30% octahedral (bulk) and 56% pyramidal (surface) ones.

Again, the results indicate that the relative intensity of these features seems to be directly related to the O_2 content during growth. Not only is the intensity of each contribution linearly proportional to the O_2 content during growth (see the inset), but also both Ni^{3+} and pyramidal Ni^{2+} parts have the same rate of increase, in detriment to the octahedral Ni^{2+} contribution.

3.3. Ni 2p x-ray absorption spectra

Figure 6 presents the experimental Ni 2p x-ray absorption spectra of samples with different growth conditions. Again, the result for the sample with no O_2 content (0%) is similar to a typical NiO spectrum [31]. The spectra given by this technique correspond to $2p^63d^8 \rightarrow 2p^53d^9$ transitions, which are separated by spin–orbit interactions into the Ni $2p_{3/2}$ and $Ni2p_{1/2}$ components, and further split by multiplet effects in two main features, A–B and A′–B′, respectively.

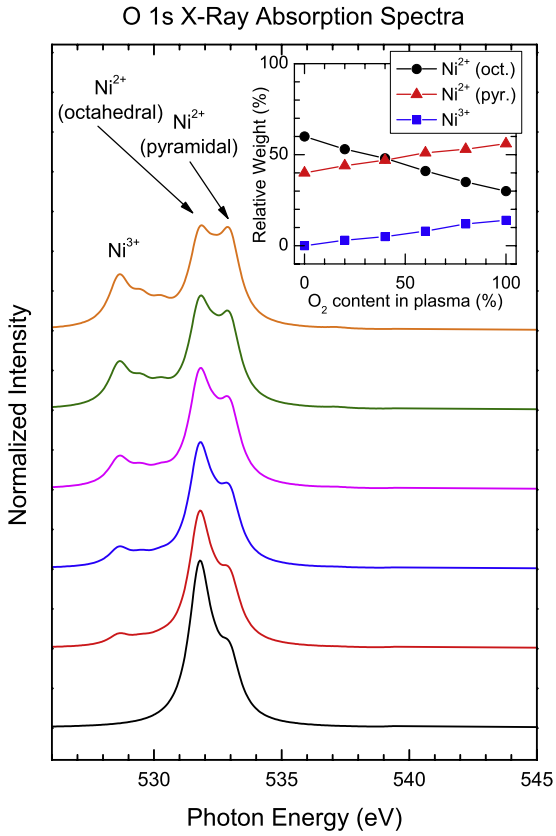

Figure 5. Calculated O 1s x-ray absorption spectra with weighted Ni^{2+} and Ni^{3+} contributions. Each weight, presented in the inset, was estimated to give the best agreement with the experimental spectra.

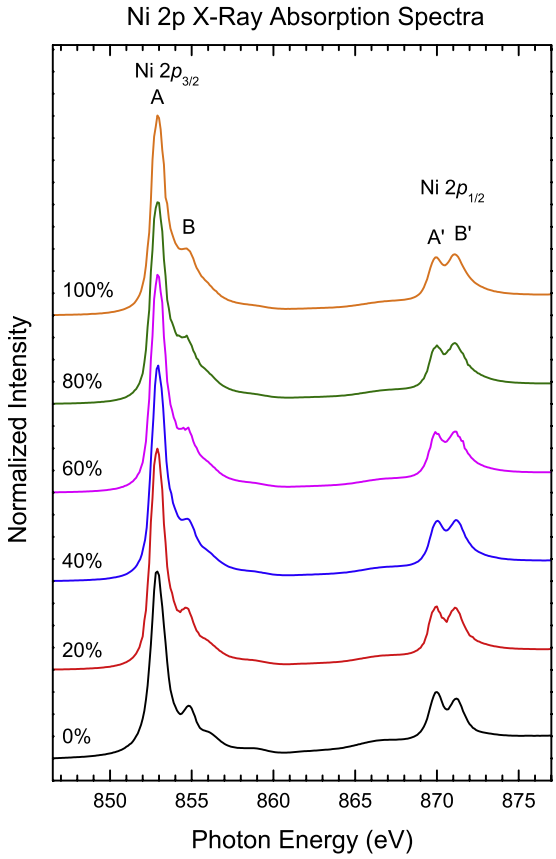

Figure 6. Ni 2p x-ray absorption spectra of NiO films as a function of O_2 content in the sputtering plasma during growth. The spectra are related to $2p^63d^8 \rightarrow 2p^53d^9$ transitions, and do not show much change as the O_2 content increases.

Surprisingly, the Ni 2p XAS spectra do not change much when samples are grown in the presence of O_2. The only difference is that the intensities of peaks B and B′ become slightly larger as the O_2 content increases. At first, this seems to contradict the results for the O 1s XAS but, as we will show below, smaller effects on this absorption edge are expected.

3.4. Ni 2p XAS calculations

In order to interpret the Ni 2p XAS results, we also did calculations using the CTM4XAS code [32]. It includes not only charge transfer configurations, but also full atomic multiplet effects, which are crucial for describing transition metal $L_{3,2}$ edges. The charge transfer and crystal field parameters are the same as those presented in table 1, and the Coulomb and exchange interactions were scaled down to 80% of their atomic values.

Figure 7 shows the Ni 2p x-ray absorption spectra calculated in the case of octahedral Ni^{2+}, pyramidal Ni^{2+}, and Ni^{3+} ions. As in the O 1s XAS spectra, the discrete final states were again convoluted with a Lorentzian and a Gaussian function.

The Ni^{2+} calculations show final states mainly related to $2p^63d^8 \rightarrow 2p^53d^9$ transitions, since the ground state is mostly formed from the $3d^8$ configuration (about 80%). In both symmetries, these transitions are split into the A–B and A′–B′ structures. This splitting is somewhat greater in the octahedral symmetry, whereas the intensity of the B′ peak is larger in the pyramidal case.

On the other hand, the Ni^{3+} spectrum is not mostly related to $2p^63d^7 \rightarrow 2p^53d^8$ transitions, but to $2p^63d^8\underline{L} \rightarrow 2p^53d^9\underline{L}$ excitations, because the ground state is mainly due to the $3d^8\underline{L}$ configuration (about 60%). As a result, the calculation is much more similar to a Ni^{2+} spectrum than to a typical high spin Ni^{3+} one [33]. Then, the spectrum is formed from a small pre-edge structure, and two main features, in each Ni $2p_{3/2}$ or Ni $2p_{1/2}$ region, which end up lying in about the same energy positions as the A–B and A′–B′ structures.

Figure 8 presents the calculated Ni 2p x-ray absorption spectra of samples with different growth conditions. The total spectra are the sums of the calculated octahedral Ni^{2+}, pyramidal Ni^{2+}, and Ni^{3+} contributions (see figure 7), whose weights are the same as in the O 1s XAS calculations, shown in the inset of figure 5.

The results confirm that, in this case, the spectra do not vary much as a function of O_2 content during growth. The only difference in the experimental spectra was a small increase in the relative intensities of peaks B and B′, which is reproduced by our calculations. Therefore, the apparent lack of influence of O_2 content in the Ni 2p edge can be attributed to the similarities in the Ni^{2+} and Ni^{3+} contributions, in

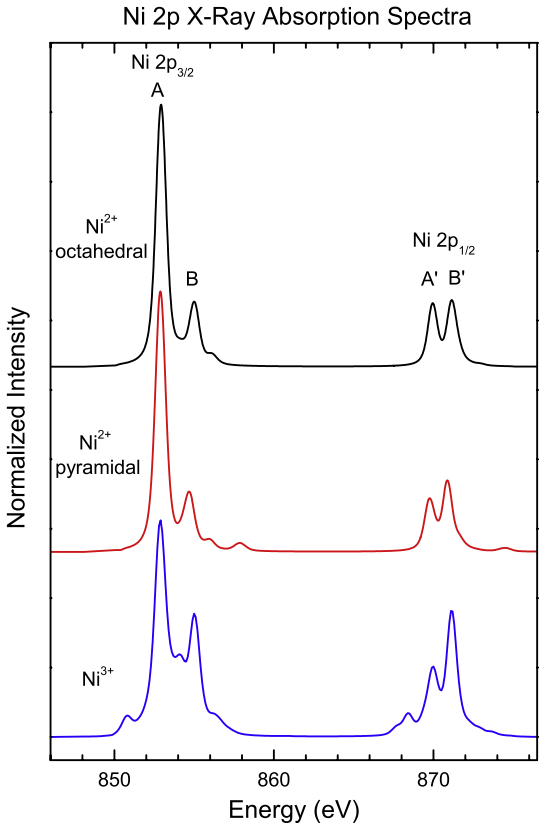

Figure 7. Calculated Ni 2p x-ray absorption spectra for octahedral Ni^{2+}, pyramidal Ni^{2+}, and Ni^{3+} ions.

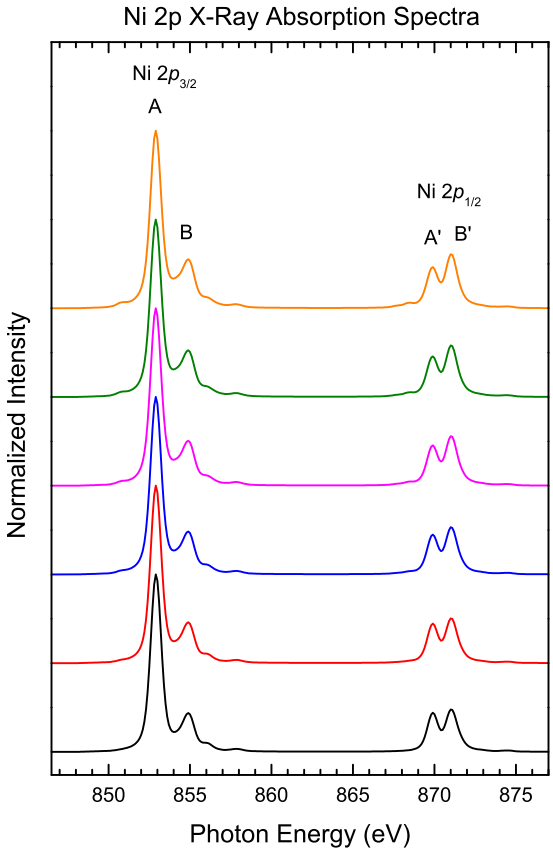

Figure 8. Calculated Ni 2p x-ray absorption spectra with weighted Ni^{2+} and Ni^{3+} contributions. The relative weights, shown in the inset of figure 5, were the same as in the O 1s XAS spectra calculations.

contrast to what we found in the O 1s edge. Please note that the small pre-edge feature in the Ni^{3+} spectrum does not contribute much to the simulation because the relative concentration of Ni^{3+} ions in the films was estimated to be at most 13%.

4. Conclusions

We have measured the O 1s and Ni 2p x-ray absorption spectra of nanocrystalline NiO thin films grown by RF magnetron sputtering with different O_2/Ar ratios in the plasma. The O 1s XAS spectra show a splitting of the peak assigned to Ni e_g states, caused by an enhancement of the surface effects due to the reduction of the crystal size, and a pre-edge peak associated with the presence of Ni vacancies. The reduction of the crystallite size has been confirmed by XRD measurements. On the other hand, electrical resistivity measurements show a correlation with the intensity of the pre-edge peak, suggesting that the electrical behaviour of the NiO films is based on the conduction by holes. Finally, the Ni 2p XAS spectra do not change much for different growth conditions. The distinct changes in each spectrum, both at the O 1s and at the Ni 2p edges, have been successfully reproduced by cluster model calculations, which showed that the Ni^{3+} and Ni^{2+} surface contributions increase linearly with the oxygen content in the plasma. Thus, the changes in this parameter during growth affect the electronic structure of these NiO films, which, in turn, can be associated with the changes in their structural and transport properties.

Acknowledgments

This work was supported by the Spanish MICINN, under projects ENE2010-21198-C04-04 and CSD2008-0023. We acknowledge the Helmholtz-Zentrum Berlin for provision of synchrotron radiation beamtime at the Optics beamline of BESSY II and would like to thank R Ovsyannikov and M Bauer for assistance. The research leading to these results has received funding from the European Community's Seventh Framework Programme (FP7/2007–2013) under grant agreement no. 312284.

References

[1] Srinivasan V and Weidner J W 1997 An electrochemical route for making porous nickel oxide electrochemical capacitors *J. Electrochem. Soc.* **144** L210–3

[2] Lang J-W, Kong L-B, Wu W-J, Luo Y-C and Kang L 2008 Facile approach to prepare loose-packed NiO nano-flakes materials for supercapacitors *Chem. Commun.* 4213–5

[3] Sato H, Minami T, Takata S and Yamada T 1993 Transparent conducting p-type NiO thin-films prepared by magnetron sputtering *Thin Solid Films* **236** 27–31

[4] Warasawa M, Watanabe Y, Ishida J, Murata Y, Chichibu S F and Sugiyama M 2013 Fabrication of visible-light-transparent solar cells using p-type NiO films by low oxygen fraction reactive RF sputtering deposition *Japan. J. Appl. Phys.* **52** 021102

[5] Yamada S, Yoshioka T, Miyashita M, Urabe K and Kitao M 1988 Electrochromic properties of sputtered nickel-oxide films *J. Appl. Phys.* **63** 2116–9

[6] Needham S A, Wang G X and Liu H K 2006 Synthesis of NiO nanotubes for use as negative electrodes in lithium ion batteries *J. Power Sources* **159** 254–7

[7] Seo S *et al* 2004 Reproducible resistance switching in polycrystalline NiO films *Appl. Phys. Lett.* **85** 5655–7

[8] Fernández-García M, Martínez-Arias A, Hanson J C and Rodríguez J A 2004 Nanostructured oxides in chemistry: characterization and properties *Chem. Rev.* **104** 4063–104

[9] Choudhary V R, Uphade B S and Mamman A S 1998 Simultaneous steam and CO_2 reforming of methane to syngas over NiO/MgO/SA-5205 in presence and absence of oxygen *Appl. Catal.* A **168** 33–46

[10] Arico A S, Bruce P, Scrosati B, Tarascon J M and Van Schalkwijk W 2005 Nanostructured materials for advanced energy conversion and storage devices *Nature Mater.* **4** 366–77

[11] Gutiérrez A, Domínguez-Cañizares G, Jiménez J A, Preda I, Díaz-Fernández D, Jiménez-Villacorta F, Castro G R, Chaboy J and Soriano L 2013 Hexagonally-arranged-nanoporous and continuous NiO films with varying electrical conductivity *Appl. Surf. Sci.* **276** 832–7

[12] Soriano L, Preda I, Gutiérrez A, Palacín S, Abbate M and Vollmer A 2007 Surface effects in the Ni 2p x-ray photoemission spectra of NiO *Phys. Rev.* B **75** 233417

[13] Mossanek R J O, Preda I, Abbate M, Rubio-Zuazo J, Castro G R, Vollmer A, Gutiérrez A and Soriano L 2011 Investigation of surface and non-local screening effects in the Ni 2p core level photoemission spectra of NiO *Chem. Phys. Lett.* **501** 437–41

[14] Preda I, Mossanek R J O, Abbate M, Álvarez L, Méndez J, Gutiérrez A and Soriano L 2012 Surface contributions to the XPS spectra of nanostructured NiO deposited on HOPG *Surf. Sci.* **606** 1426–30

[15] Palacín S, Gutiérrez A, Preda I, Hernández-Velez M, Sanz R, Jiménez J A and Soriano L 2007 Core-level electronic properties of nanostructured NiO coatings *Appl. Surf. Sci.* **254** 278–80

[16] Soriano L, Gutiérrez A, Preda I, Palacín S, Sanz J M, Abbate M, Trigo J F, Vollmer A and Bressler P R 2006 Splitting of Ni 3d states at the surface of NiO nanostructures *Phys. Rev.* B **74** 193402

[17] Preda I, Abbate M, Gutiérrez A, Palacín S, Vollmer A and Soriano L 2007 Study of the growth of NiO on highly oriented pyrolytic graphite by x-ray absorption spectroscopy *J. Electron Spectrosc. Relat. Phenom.* **156** 111–4

[18] Kuiper P, Kruizinga G, Ghijsen J, Sawatzky G A and Verweij H 1989 Character of holes in $Li_xNi_{1-x}O$ and their magnetic behavior *Phys. Rev. Lett.* **62** 221–4

[19] Van Elp J, Searle B G, Sawatzky G A and Sacchi M 1991 Ligand hole induced symmetry mixing of d^8 states in $Li_xNi_{1-x}O$, as observed in Ni 2p x-ray absorption spectroscopy *Solid State Commun.* **80** 67–71

[20] Abbate M, Zampieri G, Prado F, Caneiro A, González-Calbet J M and Vallet-Regi M 2002 Electronic structure and metal–insulator transition in $LaNiO_{3-\delta}$ *Phys. Rev.* B **65** 155101

[21] Mizokawa T, Fujimori A, Arima T, Tokura Y, Mōri N and Akimitsu J 1995 Electronic structure of $PrNiO_3$ studied by photoemission and x-ray-absorption spectroscopy: band gap and orbital ordering *Phys. Rev.* B **52** 13865

[22] Nakai S I, Mitsuishi T, Sugawara H, Maezawa H, Matsukawa T, Mitani S, Yamasaki K and Fujikawa T 1987 Oxygen K x-ray-absorption near-edge structure of alkaline-earth-metal and 3d-transition-metal oxides *Phys. Rev.* B **36** 9241

[23] Soriano L, Abbate M, Vogel J, Fuggle J C, Fernández A, González-Elipe A R, Sacchi M and Sanz J M 1993 The electronic-structure of mesoscopic NiO particles *Chem. Phys. Lett.* **208** 460–4

[24] De Groot F M F, Grioni M, Fuggle J C, Ghijsen J, Sawatzky G A and Petersen H 1989 Oxygen 1s x-ray-absorption edges of transition-metal oxides *Phys. Rev.* B **40** 5715

[25] Domínguez-Cañizares G, Gutiérrez A, Chaboy J, Díaz-Fernández D, Castro G R and Soriano L 2013 Effects of microstructure and disorder on the electronic states of nanostructured NiO *J. Mater. Sci.* submitted

[26] Kwon Y H, Chun S H, Han J H and Cho H K 2012 Correlation between electrical properties and point defects in NiO thin films *Met. Mater. Int.* **18** 1003

[27] van der Laan G, Westra C, Haas C and Sawatzky G A 1981 Satellite structure in photoelectron and Auger spectra of copper dihalides *Phys. Rev.* B **23** 4369

[28] Fujimori A and Minami F 1984 Valence-band photoemission and optical absorption in nickel compounds *Phys. Rev.* B **30** 957

[29] Bocquet A E, Mizokawa T, Morikawa K, Fujimori A, Barman S R, Maiti K, Sarma D D, Tokura Y and Onoda M 1996 Electronic structure of early 3d-transition-metal oxides by analysis of the 2p core-level photoemission spectra *Phys. Rev.* B **53** 1161

[30] van Veenendaal M A and Sawatzky G A 1993 Nonlocal screening effects in 2p x-ray photoemission spectroscopy core-level line shapes of transition metal compounds *Phys. Rev. Lett.* **70** 2459–62

[31] van der Laan G, Zaanen J, Sawatzky G A, Karnatak R and Esteva J-M 1986 Comparison of x-ray absorption with x-ray photoemission of nickel dihalides and NiO *Phys. Rev.* B **33** 4253

[32] Stavitski E and de Groot F M F 2010 The CTM4XAS program for EELS and XAS spectral shape analysis of transition metal L edges *Micron* **41** 687–94

[33] de Groot F M F, Fuggle J C, Thole B T and Sawatzky G A 1990 2p x-ray absorption of 3d transition-metal compounds: an atomic multiplet description including the crystal field *Phys. Rev.* B **42** 5459